Multilayer Separation and its Application to Separating Layers of Clouds

Igor Yanovsky[1,2], Anthony B. Davis[1], Veljko M. Jovanovic[1]

[1]Jet Propulsion Laboratory, California Institute of Technology, Pasadena, CA 91109
[2]University of California, Los Angeles, Joint Institute for Regional Earth System Science and Engineering, Los Angeles, CA 90095

UCLA CAM Report 11-68, 2011

Abstract

Remote sensing data often contains multiple layers. Many applications require layers to be decomposed before further analysis. One such application is the study of different types of clouds. Clouds affect visibility, cause turbulence, and remain the largest source of uncertainty in climate projections. In this paper, we propose a novel method for layer separation and apply it to separate multiple layers of clouds. The method is formulated as a nonlinear energy minimization problem and is solved using computationally efficient operator-splitting methods.

1. Introduction

Decomposition of two-dimensional images into a piece-wise smooth component (cartoon) and high-oscillatory component (texture) has been a rapidly developing field in recent years. Variety of proposed total variation-based methods for image decomposition rely on different metrics for modeling textures [1, 2, 12, 18, 13, 14, 6, 3, 9]. Robust models for image segmentation, many of which are variational methods [5, 11, 7], have also been effective for solving other types of classification problems in many applications. However, unlike image decomposition and segmentation problems, layer separation allows a given area (or a pixel) in an image to be attributed to none, one, or both layers. Another aspect that distinguishes the layer separation problem from image decomposition approach is the fact that one of the layers may obstruct another layer in large parts of an image, thus blocking features in an obstructed layer. An application considering multiple layers of clouds is an example where such challenges occur.

The atmosphere often consists of two or more layers of clouds. The upper clouds vary slowly in space (low oscillatory) and are strongly stratified and optically thin. On the other hand, the lower convective clouds are characterized by large optical thicknesses and have relatively sharp boundaries. They either are high oscillatory or prominently occupy large contiguous areas. Due to their inherent brightness, the lower convective clouds optically overwhelm the upper clouds (Figure 1a).

We propose to solve layer separation problem within the energy minimization framework. Our formulation is related to problems that arise frequently in compressed sensing [4, 8]. We define an energy functional and propose to minimize it using efficient variable-splitting methods.

2. Notation

We consider $m \times n$ grayscale images, represented as a vector, such as $u \in \mathbb{R}^{mn}$. Let $D^{(1)}, D^{(2)} \in \mathbb{R}^{mn \times mn}$ be the first-order forward finite difference operators in the horizontal and vertical directions, respectively. Matrix $D_i \in \mathbb{R}^{2 \times mn}$ contains the ith rows of $D^{(1)}$ and $D^{(2)}$ as its first and second rows, respectively. The total finite difference operator and the discrete gradient of u at pixel i are given by

$$D = \begin{bmatrix} D^{(1)} \\ D^{(2)} \end{bmatrix} \in \mathbb{R}^{2mn \times mn}, \qquad D_i u = \begin{bmatrix} \left(D^{(1)}u\right)_i \\ \left(D^{(2)}u\right)_i \end{bmatrix} \in \mathbb{R}^2, \quad i = 1, \ldots, mn,$$

respectively. Denote vectors $d_1, d_2 \in \mathbb{R}^{mn}$, and $d = \begin{bmatrix} d_1 \\ d_2 \end{bmatrix} \in \mathbb{R}^{2mn}$. For each pixel $i = 1, \ldots, mn$, denote $\mathbf{d}_i = \begin{bmatrix} (d_1)_i \\ (d_2)_i \end{bmatrix} \in \mathbb{R}^2$. Similarly, $b_1, b_2 \in \mathbb{R}^{mn}$, $b = \begin{bmatrix} b_1 \\ b_2 \end{bmatrix} \in \mathbb{R}^{2mn}$, and $\mathbf{b}_i = \begin{bmatrix} (b_1)_i \\ (b_2)_i \end{bmatrix} \in \mathbb{R}^2$.

3. Multilayer Separation

Let $f \in \mathbb{R}^{mn}$ represent an observed $m \times n$ grayscale image containing multiple layers. We propose a general variational framework for decomposition of image f into images u and v containing the two layers. Image u will contain a low-oscillatory layer, and image $v = f - u$ will have a layer that prominently occupies large contiguous areas and obstructs, or optically overwhelms, the low oscillatory layer in region D with boundary ∂D. We propose to consider the energy minimization problem for scale separation and disocclusion:

$$\min_{u} \; R(u) + \mu ||f - u||_* + \frac{\beta}{2} ||u - u_{\partial D}||_2^2, \tag{1}$$

where $R(u)$ is the regularization term, or a penalty on high-oscillatory components; the term $||f - u||_*$ models high-oscillatory components; $||u - u_{\partial D}||_2^2$ is the disocclusion term, where $u_{\partial D}$ denotes the value of u on ∂D. Parameters μ and β are nonnegative, with $\beta > 0$ inside D and $\beta = 0$ outside D. The region D is determined by segmenting the image $v = f - u$, containing the high-oscillatory layer. This can be achieved, for example, via minimization problem [7]:

$$\min_{c_1, c_2, \partial D} \; \int_D (v - c_1)^2 + \int_{\Omega \setminus D} (v - c_2)^2 + \gamma \int_{\partial D} ds, \tag{2}$$

where c_1 and c_2 are averages of v inside and outside D, respectively. The third term in (2) is the regularizer in the form of the length of the boundary ∂D, and $\gamma > 0$ is a parameter. Equation (2) can be re-written using level set [17, 16] formulation.

There are a variety of choices for a norm $||\cdot||_*$ modeling high oscillatory components, which include H^{-1}, BMO^{-1}, L^1, [12, 18, 9, 1], among others. The regularizing functional $R(u)$ can be in the form of bounded variation (BV) norm, measuring the total variation (TV), or can take a form of Besov norm. In particular, BV norm, originally proposed for image denoising in [19], had since been used to solve a variety of problems in image processing and computer vision. The effectiveness of the BV norm stems from its ability to preserve edges in an image.

Our choice of $R(u)$ was $||u||_{TV}$, defined as $||u||_{TV} = \sum_{i=1}^{mn} ||D_i u||$, where $D_i u \in \mathbb{R}^2$ is the discrete gradient of u at pixel i. The choice of $||\cdot||_*$ was $||\cdot||_1$. Hence, minimization problem in (1) can be written as

$$\min_u \sum_{i=1}^{mn} ||D_i u|| + \mu ||f-u||_1 + \frac{\beta}{2} ||u - u_{\partial D}||_2^2. \tag{3}$$

This formulation is related to problems that arise frequently in compressed sensing, where function u is reconstructed from a small subset of its Fourier coefficients [4, 8].

Alternating minimization algorithms, which are derived using variable-splitting techniques in optimization, were proposed in [20, 21] and [22] for TV-L^2 and TV-L^1 deconvolution problems, respectively. Also, the Split Bregman method was proposed in [10] for solving TV-L^2 denoising problems. In order to minimize (3), similar to alternating minimization and the Split Bregman methods, an additional variable $\mathbf{d}_i \in \mathbb{R}^2$ is introduced to transfer $D_i u$ out of nondifferentiable terms at each pixel, and $||\mathbf{d}_i - D_i u||_2^2$ is penalized in Bregman sense. Since L^1 term in equation (3) is not quadratic in u, the original Split Bregman method needs to be generalized to solve TV-L^1 minimization subproblem. Similar to the non-Bregman alternative minimization formulation for deconvolution in [22], we extend the Split Bregman method to solve TV-L^1 subproblem in (3) as follows. We consider the following minimization problem where an additional variable $z \in \mathbb{R}^{mn}$ is introduced to approximate $u - f$ in Bregman sense. Hence, we rewrite the minimization problem for (3) as

$$\begin{aligned} \min_{u,\mathbf{d},z} \quad & \sum_i ||\mathbf{d}_i||_2 + \frac{\lambda}{2} \sum_i ||\mathbf{d}_i - D_i u - \mathbf{b}_i||_2^2 \\ & + \mu ||z||_1 + \frac{\alpha}{2} ||z - (u-f) - w||_2^2 + \frac{\beta}{2} ||u - u_{\partial D}||_2^2, \end{aligned} \tag{4}$$

where λ and α are nonnegative parameters, and variables $\mathbf{b}_i$ and w are chosen through Bregman iterations [23, 15]:

$$\begin{aligned} \mathbf{b}_i &\leftarrow \mathbf{b}_i + (D_i u - \mathbf{d}_i), \\ w &\leftarrow w + (u - f - z). \end{aligned}$$

For a fixed u, the minimization problem for $\mathbf{d}_i$ is

$$\mathbf{d}_i^* = \arg\min_{\mathbf{d}_i} \sum_i ||\mathbf{d}_i||_2 + \frac{\lambda}{2} \sum_i ||\mathbf{d}_i - D_i u - \mathbf{b}_i||_2^2,$$

which can be explicitly solved for $\mathbf{d}_i$ using a generalized shrinkage formula [20]:

$$\mathbf{d}_i \;=\; \max\left(||D_i u + \mathbf{b}_i||_2 - \frac{1}{\lambda}, 0\right) \frac{D_i u + \mathbf{b}_i}{||D_i u + \mathbf{b}_i||_2}.$$

The minimization problem for z is

$$z^* \;=\; \arg\min_z \;\; \mu||z||_1 \;+\; \frac{\alpha}{2}||z - (u - f) - w||_2^2,$$

with a minimizer given by the one-dimensional shrinkage:

$$z \;=\; \max\left\{|u - f + w| - \frac{\mu}{\alpha}, 0\right\} \operatorname{sign}(u - f + w).$$

For a fixed $\mathbf{d}$ and z, the minimization problem (4) for u is quadratic in u:

$$u^* \;=\; \arg\min_u \;\; \sum_i ||\mathbf{d}_i - D_i u - \mathbf{b}_i||_2^2 \;+\; \frac{\alpha}{\lambda}||z - (u - f) - w||_2^2 \;+\; \frac{\beta}{\lambda}||u - u_{\partial D}||_2^2.$$

The minimizer for u is given by the normal equations:

$$\begin{aligned}\left((D^{(1)})^T D^{(1)} + (D^{(2)})^T D^{(2)} + \frac{\alpha - \beta}{\lambda} I\right) u \;&=\; (D^{(1)})^T (b_1 - d_1) + (D^{(2)})^T (b_2 - d_2) \\ &\quad + \frac{\alpha}{\lambda}(f + z - w) - \frac{\beta}{\lambda} u_{\partial D},\end{aligned}$$

which, similar to [20], can be solved using the fast Fourier transform:

$$u \;=\; \left(\frac{\widehat{D^{(1)}} \cdot \widehat{(b_1 - d_1)} + \widehat{D^{(2)}} \cdot \widehat{(b_2 - d_2)} + \frac{\alpha}{\lambda}\widehat{(f + z - w)} - \frac{\beta}{\lambda}\widehat{u_{\partial D}}}{\widehat{D^{(1)}} \cdot \widehat{D^{(1)}} + \widehat{D^{(2)}} \cdot \widehat{D^{(2)}} + \frac{\alpha - \beta}{\lambda}}\right)^{\vee},$$

where $\wedge$ denotes Fourier transform, $\vee$ denotes inverse Fourier transform, and $I \in \mathbb{R}^{mn \times mn}$ is an identity matrix.

4. Results

There is a rich source of multi-angle multispectral data, containing a wide variety of scenes, which is available to test our methodology. The data is acquired by the Multi-Angle Imaging Spectro-Radiometer (MISR), which has nine digital cameras, pointing at different angles, and gathering data in four different spectral bands of the visible spectrum. Each region on Earth's surface is successively captured by all nine cameras in blue, green, red, and near-infrared wavelengths.

We consider a single-channel multilayer image shown on Figure 1(a). This image was generated by combining red, green, and blue channels of a real multichannel image to create a grayscale image. As noticeable on this image, the upper cirrus clouds vary slowly in space and are optically thin. On the other hand, the lower convective clouds are optically thick, have relatively sharp boundaries, and optically overwhelm the upper clouds. Figures 1(b,c) show results obtained after decomposing this image into low-oscillatory cirrus layer, u, and optically thick convective cloud layer, v.

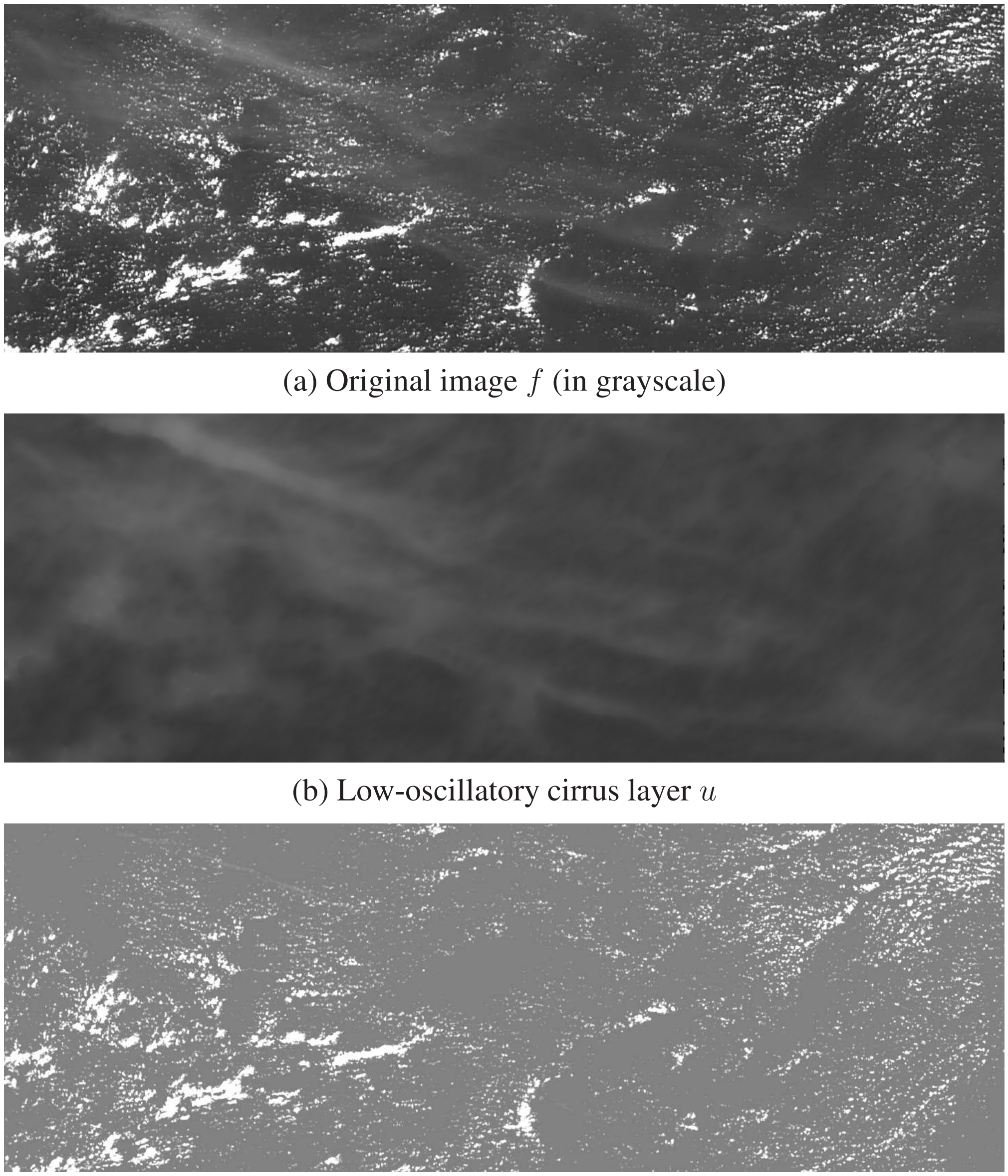

(a) Original image f (in grayscale)

(b) Low-oscillatory cirrus layer u

(c) Convective cloud layer v

Figure 1. Layer separation of (a) a single-channel single-angle image f into (b) low-oscillatory cirrus layer u and (c) optically thick convective clouds v.

Acknowledgements

The research was carried out at the Jet Propulsion Laboratory, California Institute of Technology, under a contract with the National Aeronautics and Space Administration. The authors would like to thank David Diner and Luminita Vese for their helpful discussions and comments.

References

[1] S. Alliney. Digital filters as L1-norm regularizers. *Sixth Multidimensional Signal Processing Workshop*, page 105, 1989.

[2] S. Alliney. Digital filters as absolute norm regularizers. *IEEE Transactions on Signal Processing*, 40(6):1548–1562, 1992.

[3] A. Buades, T. Le, J.-M. Morel, and L. Vese. Fast cartoon + texture image filters. *IEEE Transactions on Image Processing*, 19(8):1978–1986, 2010.

[4] E. Candes, J. Romberg, and T. Tao. Robust uncertainty principles: Exact signal reconstruction from highly incomplete frequency information. *IEEE Transactions on Information Theory*, 52(2):489–509, 2006.

[5] V. Caselles, R. Kimmel, and G. Sapiro. Geodesic active contours. *International Journal of Computer Vision*, 22(1):61–79, 1997.

[6] T. Chan and S. Esedoglu. Aspects of total variation regularized L1 function approximation. *SIAM Journal on Applied Mathematics*, 65(5):1817–1837, 2005.

[7] T. Chan and L. Vese. Active contours without edges. *IEEE Transactions on Image Processing*, 10(2):266–277, 2001.

[8] D. Donoho. Compressed sensing. *IEEE Transactions on Information Theory*, 52(4):1289–1306, 2006.

[9] J. Garnett, P. Jones, T. Le, and L. Vese. Modeling oscillatory components with the homogeneous spaces $B\dot{M}O^{-\alpha}$ and $\dot{W}^{-\alpha,p}$. *Pure and Applied Mathematics Quarterly*, 7(2):275–318, 2011.

[10] T. Goldstein and S. Osher. The split bregman method for L1-regularized problems. *SIAM J. Imaging Sci.*, 2(2):323–343, 2009.

[11] S. Kichenassamy, A. Kumar, P. Olver, A. Tannenbaum, and A. Yezzi. Conformal curvature flows: From phase transitions to active vision. *Archive for Rational Mechanics and Analysis*, 134(3):275–301, 1996.

[12] Y. Meyer. *Oscillating patterns in image processing and nonlinear evolution equations*. American Mathematical Society, Providence, RI, 2001.

[13] M. Nikolova. Minimizers of cost-functions involving nonsmooth data-fidelity terms. Application to the processing of outliers. *SIAM Journal on Numerical Analysis*, 40(3):965–994, 2003.

[14] M. Nikolova. A variational approach to remove outliers and impulse noise. *Journal of Mathematical Imaging and Vision*, 20:99–120, 2004.

[15] S. Osher, M. Burger, D. Goldfarb, J. Xu, and W. Yin. An iterative regularization method for total variation-based image restoration. *Multiscale Modeling & Simulation*, 4(2):460–489, 2005.

[16] S. Osher and R. Fedkiw. *Level Set Methods and Dynamic Implicit Surfaces*. Applied Mathematical Sciences. Springer-Verlag, New York, 2003.

[17] S. Osher and J. Sethian. Fronts propagating with curvature dependent speed: Algorithms based on Hamilton-Jacobi formulations. *Journal of Computational Physics*, 79:12–49, 1988.

[18] S. Osher, A. Sole, and L. Vese. Image denoising and decomposition with total variation minimization and oscillatory functions. *Multiscale Modeling & Simulation*, 1(3):349–370, 2003.

[19] L. Rudin, S. Osher, and E. Fatemi. Nonlinear total variation based noise removal algorithms. *Physica D*, 60:259–268, 1992.

[20] Y. Wang, J. Yang, W. Yin, and Y. Zhang. A new alternating minimization algorithm for total variation image reconstruction. *SIAM J. Imaging Sci.*, 1(3):248–272, 2008.

[21] J. Yang, W. Yin, Y. Zhang, and Y. Wang. A fast algorithm for edge-preserving variational multichannel image restoration. *SIAM J. Imaging Sci.*, 2:569–592, 2009.

[22] J. Yang, Y. Zhang, and W. Yin. An efficient TVL1 algorithm for deblurring multichannel images corrupted by impulsive noise. *SIAM J. Sci. Comput.*, 31(4):2842–2865, 2009.

[23] W. Yin, S. Osher, D. Goldfarb, and J. Darbon. Bregman iterative algorithms for L1-minimization with applications to compressed sensing. *SIAM J. Imaging Sci.*, 1(1):143–168, 2008.